CHARGE STATE STUDY OF FLUORINE K X RAYS FOLLOWING A FLUORINE-NEON COLLISION

304

by

PHILIP L. PEPMILLER

B.S., Florida State University, 1977

A MASTER'S THESIS

submitted in partial fulfillment of the

requirements for the degree

MASTER OF SCIENCE

Department of Physics

KANSAS STATE UNIVERSITY

Manhattan, Kansas

1980

Approved by:

Patrick Richard

Major Professor

THIS BOOK
CONTAINS
NUMEROUS PAGES
WITH ILLEGIBLE
PAGE NUMBERS
THAT ARE CUT OFF,
MISSING OR OF POOR
QUALITY TEXT.

THIS IS AS RECEIVED
FROM THE
CUSTOMER.

THIS BOOK
CONTAINS
NUMEROUS PAGES
WITH THE ORIGINAL
PRINTING BEING
SKEWED
DIFFERENTLY FROM
THE TOP OF THE
PAGE TO THE
BOTTOM.

THIS IS AS RECEIVED
FROM THE
CUSTOMER.

TABLE OF CONTENTS

LIST OF FIGURES AND TABLES

ACKNOWLEDGEMENTS

Thanks are due in varying degrees to various people I have been associated with.

To Pat Richard, for his patience in the face of numerous questions which must seem trivial.

To James Hall, Joal Newcomb, Hiro Tawara, and Mititaka Terasawa, who helped with the data collection and interpretation.

To Dea Richard for some typing, but mainly knowing how to keep things running smoothly.

To my parents for their love and support even when I deserved less.

To Trea.

I also acknowledge financial support of the United States Department of Energy, Division of Chemical Sciences.

I. INTRODUCTION

The study of K x-rays from multiply ionized ions began with the work of Coates[1] who noted that targets bombarded with 2.4 MeV mercury ions emitted x-rays which were neither characteristic of the projectile nor of the target. This was in contradiction to the works of previous researchers who had shown that the radiation had energies which followed a definite law first obtained by Mosley[2], dependent upon the square of the nuclear charge of the emitting ion. It was not until thirty years later that further study of these noncharacteristic x-rays was resumed, when Specht[3], Richard[4], and Burch[5] showed that the energies of various K x-ray lines were shifted to higher energies when the x-ray was produced as a result of a heavy-ion atom collision. It was postulated that the change in energy of the K x-ray was due to multiple ionization of the L-shell simultaneous with K ionization. It was also suggested by Richard[4] that the study of spectra with a high resolution spectrometer should confirm the multiple ionization hypothesis by resolving the individual transitions which make up the Kβ line. Subsequent measurements by Knudson[6] and Burch[7] using a Bragg crystal spectrometer showed that the K x-ray spectra could be resolved into various components in accordance with the degree of multiple ionization of the emitting ion.

Most investigations of K x-rays have involved the measurement of the x-ray yield from a solid target after its interaction with a beam of ions. The straightforwardness of the approach and the ease of the experimental setup has contributed strongly to the popularity of this method. A beam of ions is directed onto a target which is angled (usually 45°) to the axis

of the beam. An x-ray detector faces the front of the target to record the x-rays emitted. As an ion enters the target, it quickly adjusts the number of its bound electrons to some equilibrium value dependent upon its energy, nuclear charge, and target material, minimizing the importance of the charge selected for the incident beam. During the ion's passage, each target atom is subjected to, at most, one collision since the beam currents and focusing normally used will allow sufficient time for the target atom to de-excite before the arrival of the next ion. Any collision which results in a K-shell vacancy also has a non-negligible probability of leaving the target ion with one or more L-shell holes. The number and the probability distribution are found to obey binomial statistics. The peak of the distribution is dependent upon the incident Z, but the resultant x-ray spectra is complicated by still other effects. Since the target atom of a solid is either bound in its lattice or to its neighboring atom, the chemical configuration of the target will affect the distribution of x-ray energies due to electrons of neighboring atoms filling the target ion's holes before de-excitation can take place.[8,9,10,11] Additionally, the ion may adjust its vacancy configuration internally and independently of the surrounding medium before emitting an x-ray.[12] The complications produced by these effects necessitates altering the fluorescence yield from the single K, no other vacancy value, to an average fluorescence yield, $\bar{\omega}$, to calculate the total cross sections for vacancy production.

Another method of target x-ray investigation is to use a gas target material contained within a cell. The similarities between this and a solid target are numerous. The target atom once again undergoes a single collision, producing a statistical distribution of vacancies, which may rearrange internally before x-ray emission. The chemical state of the target affects the filling of outer shells, similiarly to the solids

studied[13,14] requiring the generalization to an average fluorescence yield. However, since it is possible to have an ion arrive at the target atom without previously encountering other target atoms, the charge state of the incident ion can be selected. This has been shown to be important as both the projectile and target x-ray yields increase markedly with the charge state of the incident ion.[15,16,17]

For certain processes, such as the lifetimes of certain states and charge state dependences, it is more advantageous to study the projectile rather than the target x-rays. As an ion passes through a solid target, it is subjected to multiple collisions with the target atoms which makes the study of the x-rays emitted during its transition difficult. After the ion leaves the target, detection of x-rays at several points can yield accurate information from which the lifetimes of excited states can be determined. If the beam target interaction region is modified so that a gas target is available, a multitude of additional information can be extracted. It then becomes possible to vary the gas pressure until single collision events are dominant, thus, both the initial configuration which is determined by the beam selection, and the final configuration, as observed by the x-ray detector, are known. This versatility was put to use by Hopkins[17] and more recently by Tawara[18] to study electron excitation, ionization and electron capture by various projectiles on noble gases.

The purpose of this thesis is to continue the study of projectile x-rays resulting from electron excitation, ionization and electron capture after collision with a gas target. Various charge states of a 15 MeV fluorine beam were directed onto a neon target. The x-rays emitted by the

fluorine were analyzed by a high resolution four-inch Bragg curved crystal spectrometer to yield information as to the populations of resulting charge states and more explicitly, the electronic configurations resulting from the collision.

II. PROCEDURE

The Tandem

For this experiment, fluorine ions were accelerated to an energy of 15 MeV by the KSU EN tandem Van de Graaff accelerator, then momentum analyzed by a 90° bending magnet (see Fig. 1). The lower charge states, F^{2+} through F^{5+}, were obtained by gas stripping in the terminal of the tandem, producing currents of from 100 to 300 nanoamperes at the Faraday cup. The cross sections for producing the higher charge states, F^{6+} through F^{9+}, are too small to produce a useable beam in this manner, so a poststripper was necessary. The 15 MeV beam was allowed to pass through a thin ($5\mu g/cm^2$) carbon foil. The beam exiting this foil has a distribution of charge states, any of which may be chosen for study by suitably adjusting the magnetic field of the switching magnet. Using this arrangement, beam currents of from 2 to 400 nA in charge states 6^+ to 9^+ were focused into the Faraday cup.

The Chamber

The target chamber is shown schematically in Figure 2. The fluorine beam entered the gas cell after being collimated by the adjustable 4 jaw and the entrance aperture (1.8mm diameter), then exited the gas cell through the exit aperture (2.0mm diameter) to be collected by the Faraday cup. The neon target gas was introduced into the interaction region by a single stage regulator and needle valve arrangement. The gas pressure in the cell was monitored by a Baratron pressure gauge and was constant to within 5% with no further regulation of input flow necessary. The vacuum

Figure 1: Schematic of the Kansas State University Tandem Van de Graaff Accelerator

THIS BOOK CONTAINS NUMEROUS PAGES WITH DIAGRAMS THAT ARE CROOKED COMPARED TO THE REST OF THE INFORMATION ON THE PAGE.

THIS IS AS RECEIVED FROM CUSTOMER.

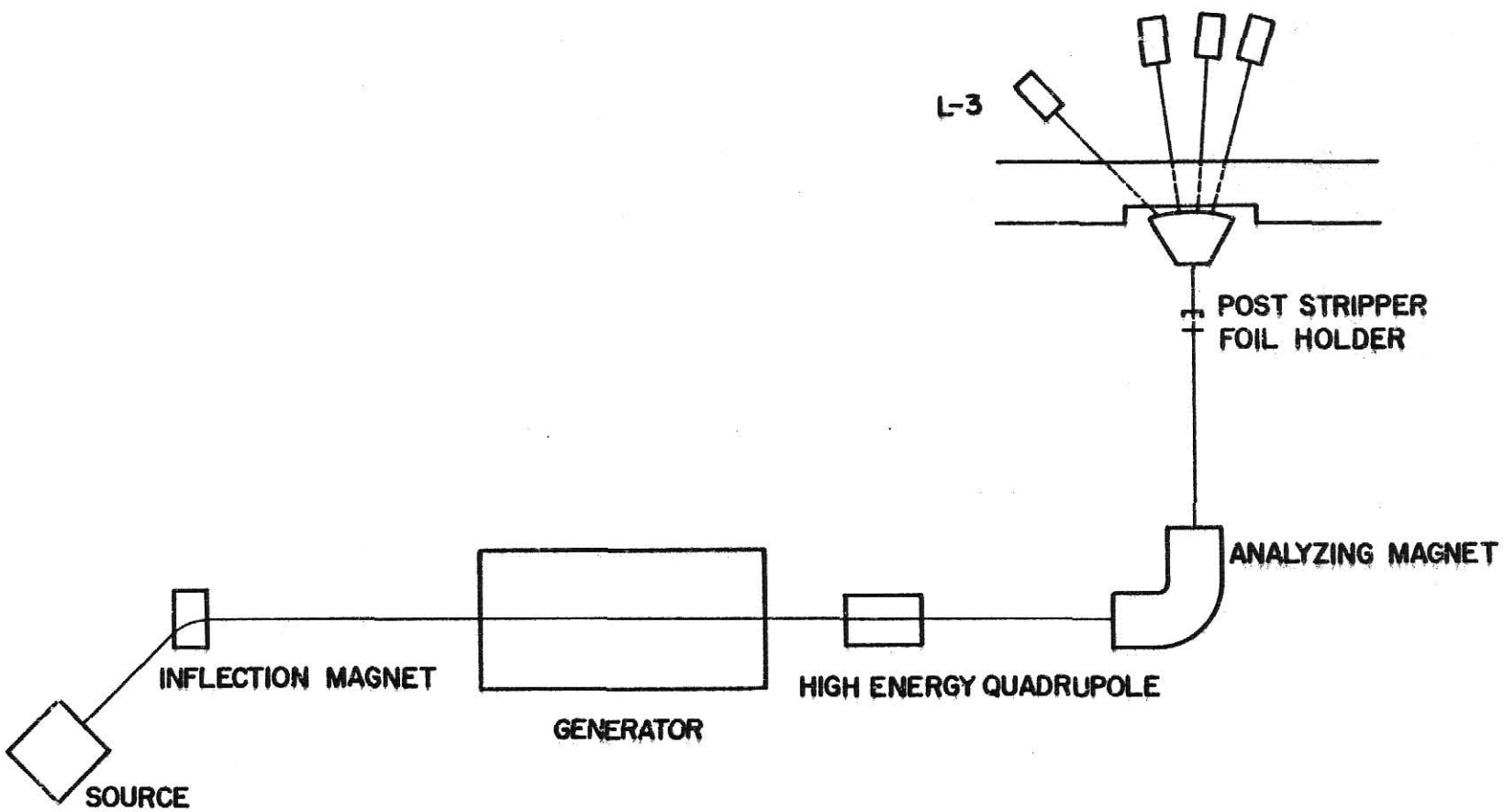

A SCHEMATIC DIAGRAM OF THE KANSAS STATE TANDEM Van de Graaff ACCELERATOR

Figure 2: Diagram of the experimental chamber used in this experiment

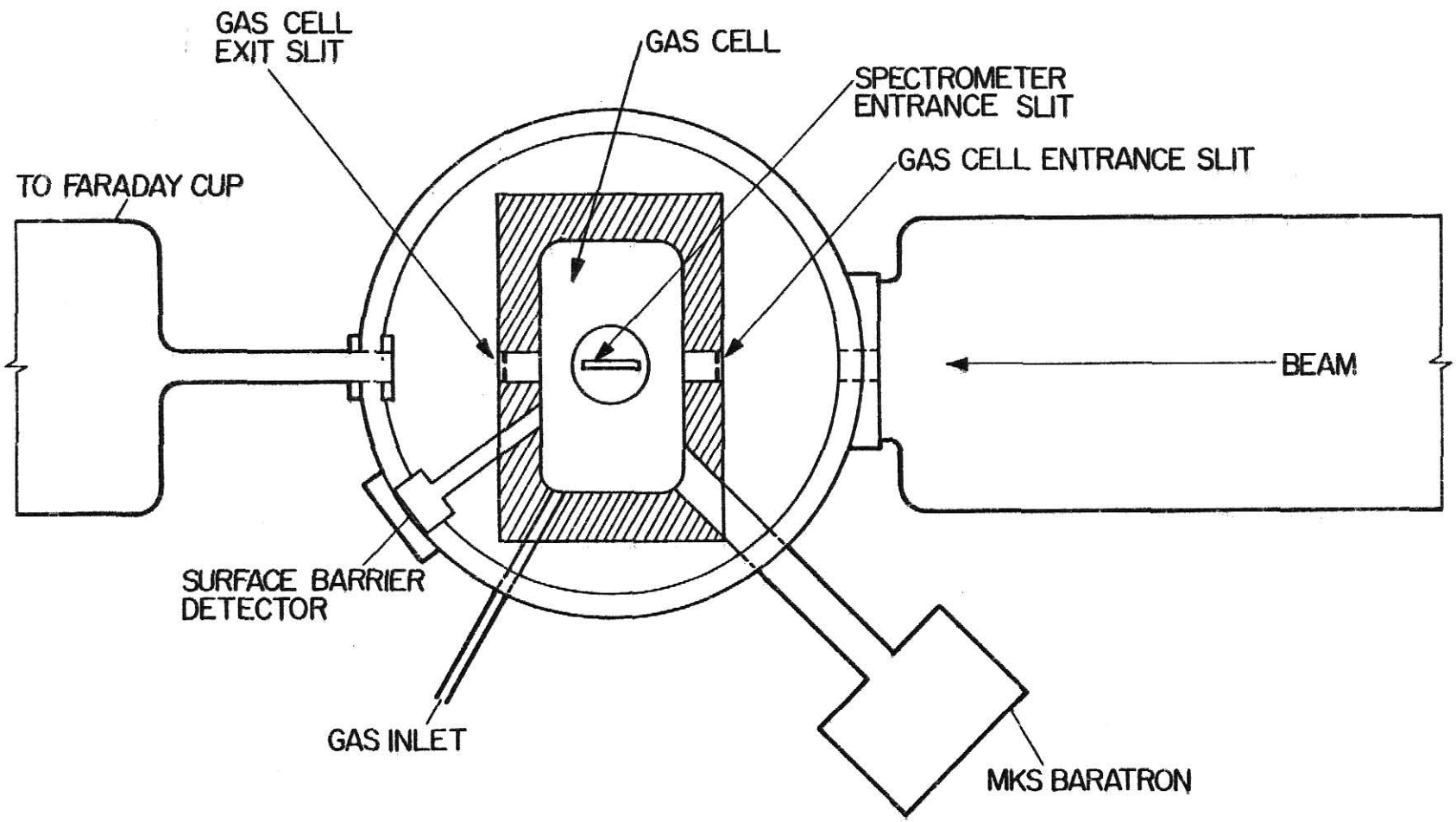
GAS CELL
EXIT SLIT
GAS CELL
SPECTROMETER
ENTRANCE SLIT
GAS CELL ENTRANCE SLIT
TO FARADAY CUP
BEAM
SURFACE BARRIER
DETECTOR
GAS INLET
MKS BARATRON

ILLEGIBLE DOCUMENT

THE FOLLOWING DOCUMENT(S) IS OF POOR LEGIBILITY IN THE ORIGINAL

THIS IS THE BEST COPY AVAILABLE

in the beam line was maintained by two 6" oil diffusion pump/mechanical roughing pump stations, which kept the residual pressure in the beam line to between 10^{-6} and 10^{-7} torr. A third pumping station, consisting of a 4" oil diffusion pump and mechanical roughing pump, was used to pump the spectrometer chamber.

A problem often encountered in gas target experiments is contamination of the target. Nitrogen, oxygen, and argon contained in the gas cell can significantly alter the x-ray yields of the fluorine ions. These impurities must be monitored in order to insure the accuracy of the data collected. This was accomplished by a surface barrier detector which was placed in the interaction region at 35^{o} to the beam axis. Fluorine ions elastically scattered from the gasses in the cell, and the recoil of these gasses from the fluorine ion impact, were recorded by the detector. A typical spectrum of the particle detector is shown in Figure 3, along with an energy calibration and the calculated energies of suspected contaminant reaction products.

The x-rays produced due to collisions in the gas cell were wavelength analyzed by an ARL curved crystal spectrometer. The x-rays entered the spectrometer through the spectrometer slit (.38 X 12.5mm) which acted as a collimator for the x-rays, and as a baffle to the target gas. The x-rays were then reflected by a rubidium acetate phosphate (RAP) Johansson focusing crystal.[19] This type of crystal has been aligned, machined, and bent, such that the crystal planes will form concentric circles with a radius 2R. Referring to Figure 4, if a source is placed at S, and a detector at D, such that arc OD equals arc OS, the crystal will give exact focusing. The proof of this follows rather quickly. Choose any two points A and B, and connect them to O, S, D as shown. The point O is the center of

Figure 3: Typical 15 MeV F on Ne particle spectrum

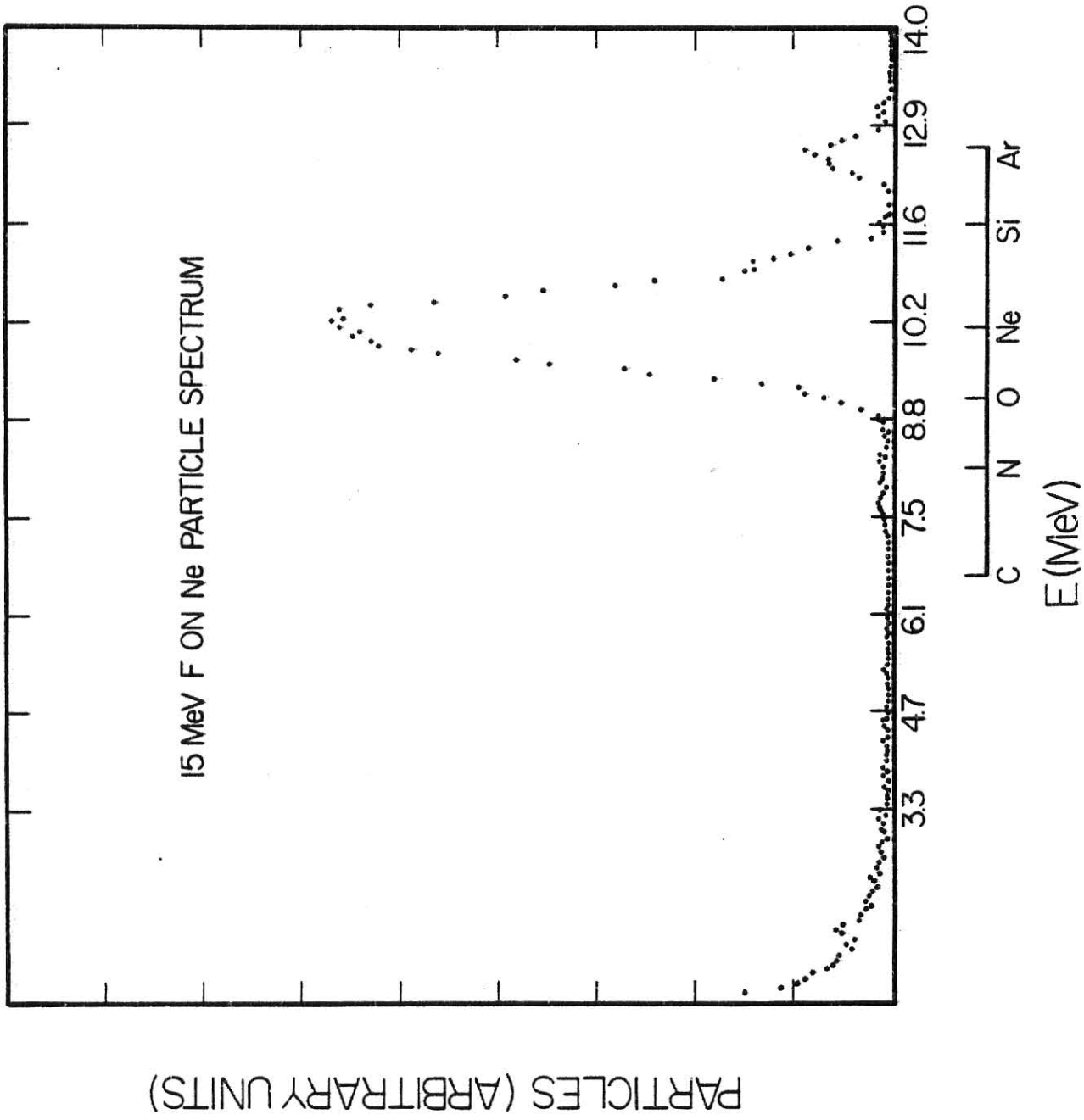
15 MeV F ON Ne PARTICLE SPECTRUM
PARTICLES (ARBITRARY UNITS)
3.3
4.7
6.1
7.5
8.8
10.2
11.6
12.9
14.0
C
N
O
Ne
Si
Ar
E(MeV)

Figure 4: Diagram of the geometry of a Johansson crystal

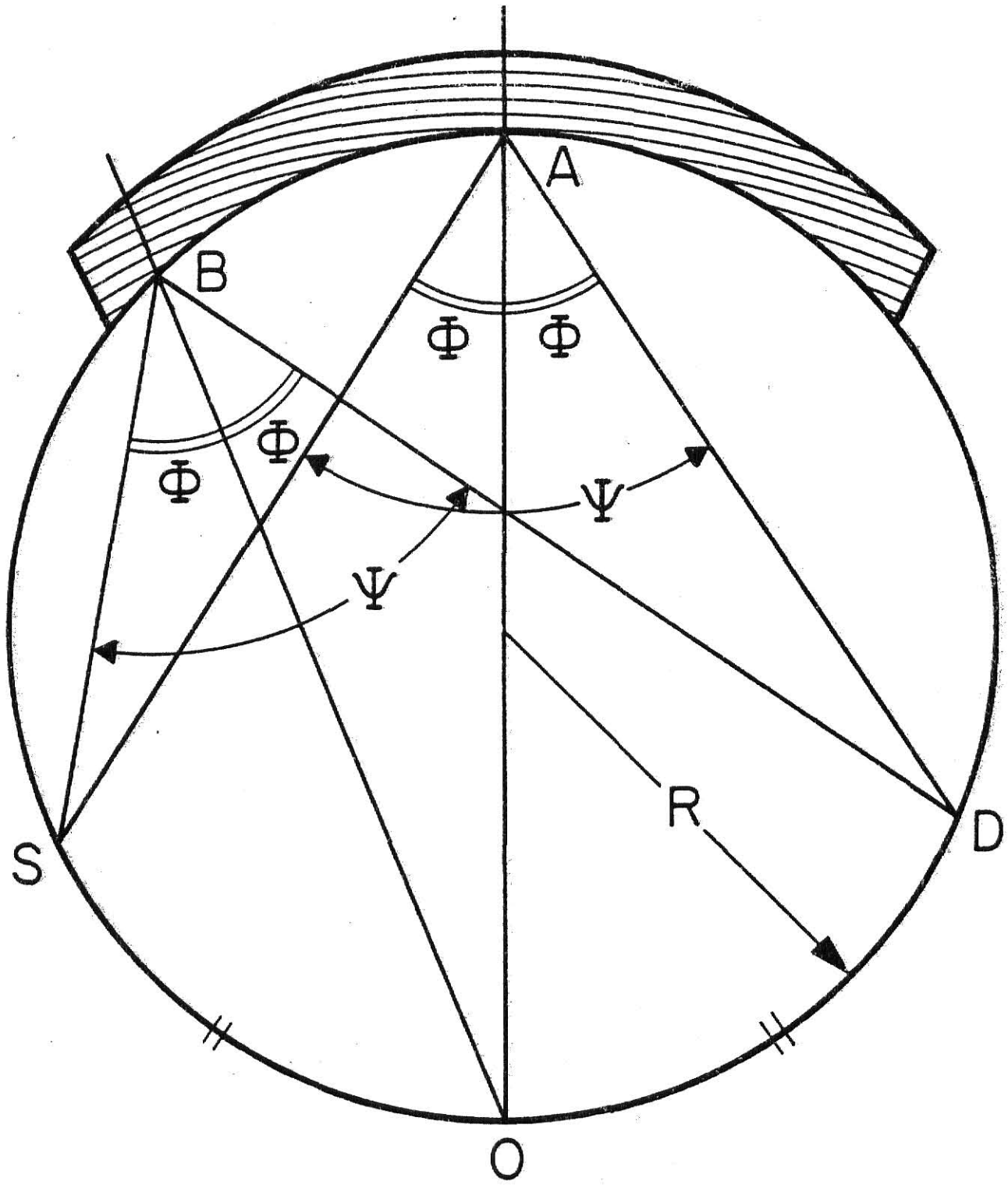
A
B
Φ
Φ
Φ
Φ
Ψ
Ψ
R
S
D
O

the concentric planes of the crystal, so OA and OB are perpendicular to the crystal planes. All of the angles Φ are equal, since any two chords subtending equal arcs form equal angles. Thus, the angle of incidence equals the angle of reflection, and the reflected x-rays will interfere constructively, giving exact focusing. The x-rays focused by the crystal enter the flow mode proportional counter which uses a P-10 (90% argon, 10% methane) detector gas mixture at atmospheric pressure contained behind a thin mylar $(C_{10}H_8O_4)_n$ window.

The Electronics

The output from the proportional counter is treated as a binary pulse, that is, we determine the energy of the incident x-ray purely on knowledge of the angle of the Johansson crystal at the time of the x-ray. This required accurate control of the spectrometer stepping motor which positions the crystal and detector, and a computer interface capable of many interdependent functions. (Figure 5).

At the start of a scan of energies of interest an enable signal is produced which gates on a series of scalers as an Analog-to-Digital Converter (ADC). The charge accumulated by the Faraday cup is digitalized by a Brookhaven Instruments Corporation Current Integrator, whose output is proportional to the digitalizer scale and the current on the Faraday cup. This signal is fed to a scaler and to the Q charge input of the computer interface. This digitalized charge is accumulated until a preset limit is reached, at which time, the spectrometer is instructed to move to the next wavelength/angle setting, the number of motor steps is noted by a scaler, the accumulated charge register is reset to zero, and the process is repeated. During the time the spectrometer is being stepped, a gate off signal is

Figure 5: Schematic of the electronics used in this experiment

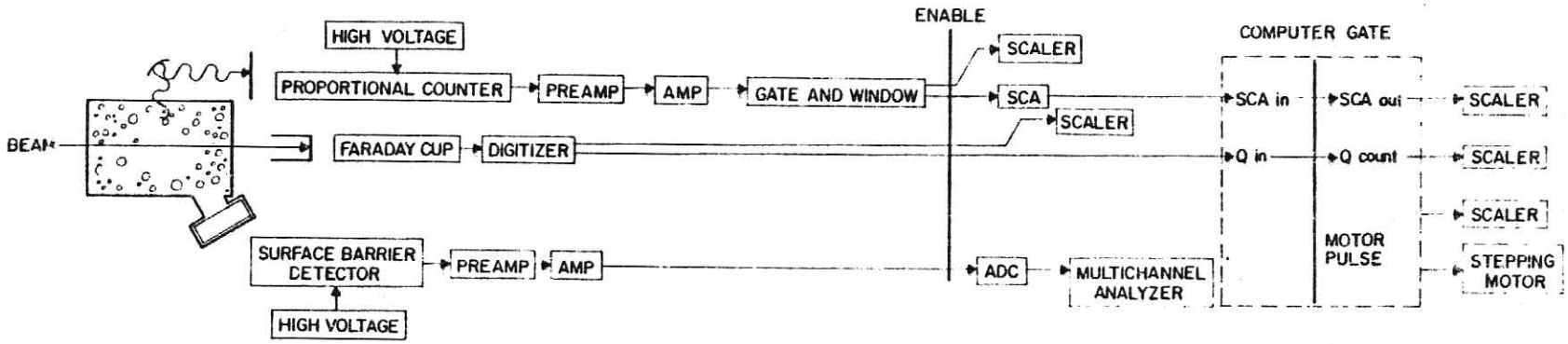
HIGH VOLTAGE
PROPORTIONAL COUNTER
PREAMP
AMP
GATE AND WINDOW
ENABLE
SCALER
SCA
SCALER
COMPUTER GATE
SCA in
SCA out
SCALER
BEAM
FARADAY CUP
DIGITIZER
Q in
Q count
SCALER
SCALER
MOTOR PULSE
STEPPING MOTOR
SURFACE BARRIER DETECTOR
PREAMP
AMP
ADC
MULTICHANNEL ANALYZER
HIGH VOLTAGE

applied to the input Q signal, and therefore, inhibiting the signal output to the scaler. The proportional counter output, having been suitably amplified and an energy window set to eliminate noise pulses, is recorded by a scaler and enters into the SCA (single channel analyzer) input of the computer interface. All the counts taken during a particular spectrometer setting are accumulated in a single computer channel, with data from the next setting in the next channel, and so on. The SCA input is gated off during the spectrometer movement and thereby, inhibiting the signal output to the scaler, as in the care of the Q count signal. The output from the recoil monitor is energy dependent, so its signal is amplified and fed into an ADC, and the spectra recorded by a multichannel analyzer. At the end of a run, the enable signal is discontinued, gating off all scalers and the ADC. The x-ray and particle spectra were recorded on magnetic tape for analysis and reference, and the displays of the scalers noted in the run book.

III. RESULTS

A major advantage inherent in the use of a gas target is the ability of the researcher to minimize the number of incident ions which undergo multiple collisions within the target chamber. Figure 6 gives the results of a pressure dependence study which shows the yields of various projectile x-ray transitions (see next section) as a function of the target gas pressure. The yields are shown to be fairly linear with pressure through 40 millitorr after which the effects of multiple collisions become significant.

The ratio of the ^3P to ^1P x-ray yields is plotted versus pressure in Figure 7. The nonlinearity of this ratio was previously reported to be due to quenching of the metastable ^3P state by Fortner.[20]

The Spectra

Figures 8 and 9 show the relative x-ray yields as a function of the incident fluorine ion charge state. The following paragraphs contain identification and production mechanisms for the various peaks.[21] A gradual shift is observed toward higher final charge states with a gradual increase total cross sections for the low (F^{2+} - F^{6+}) incident charge states. The increase becomes quite pronounced for the high (F^{7+} - F^{9+}) charge state incident ions.

F^{2+} ($1s^2 2s^2 2p^3$)

The first discernible peak, at 702 eV, results from one K-shell and one L-shell electron being ionized, forming an intermediate $1s2s^2 2p^2$ configuration, which decays to a $1s^2 2s^2 2p$ final state. The next peak can

Figure 6: Ne pressure dependence of F^{3+} projectile K X-ray yields

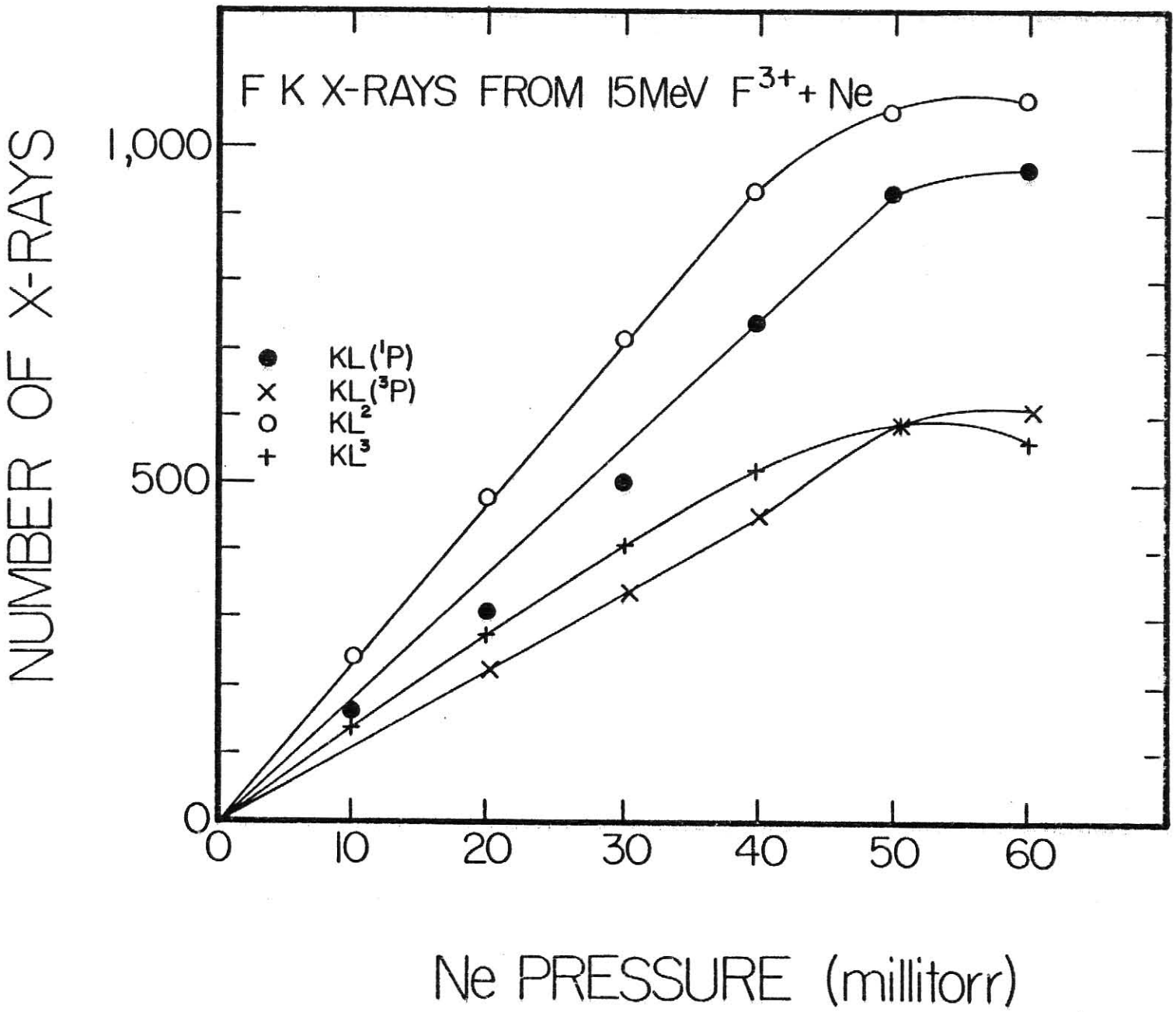
F K X-RAYS FROM 15MeV F^{3+} + Ne
NUMBER OF X-RAYS
1,000
500
0
KL(^{1}P)
KL(^{3}P)
KL^2
KL^3
0
10
20
30
40
50
60
Ne PRESSURE (millitorr)

Figure 7: Ratio of $1s2p(^3P)$ to $1s2p(^1P)$ X-rays as a function of pressure

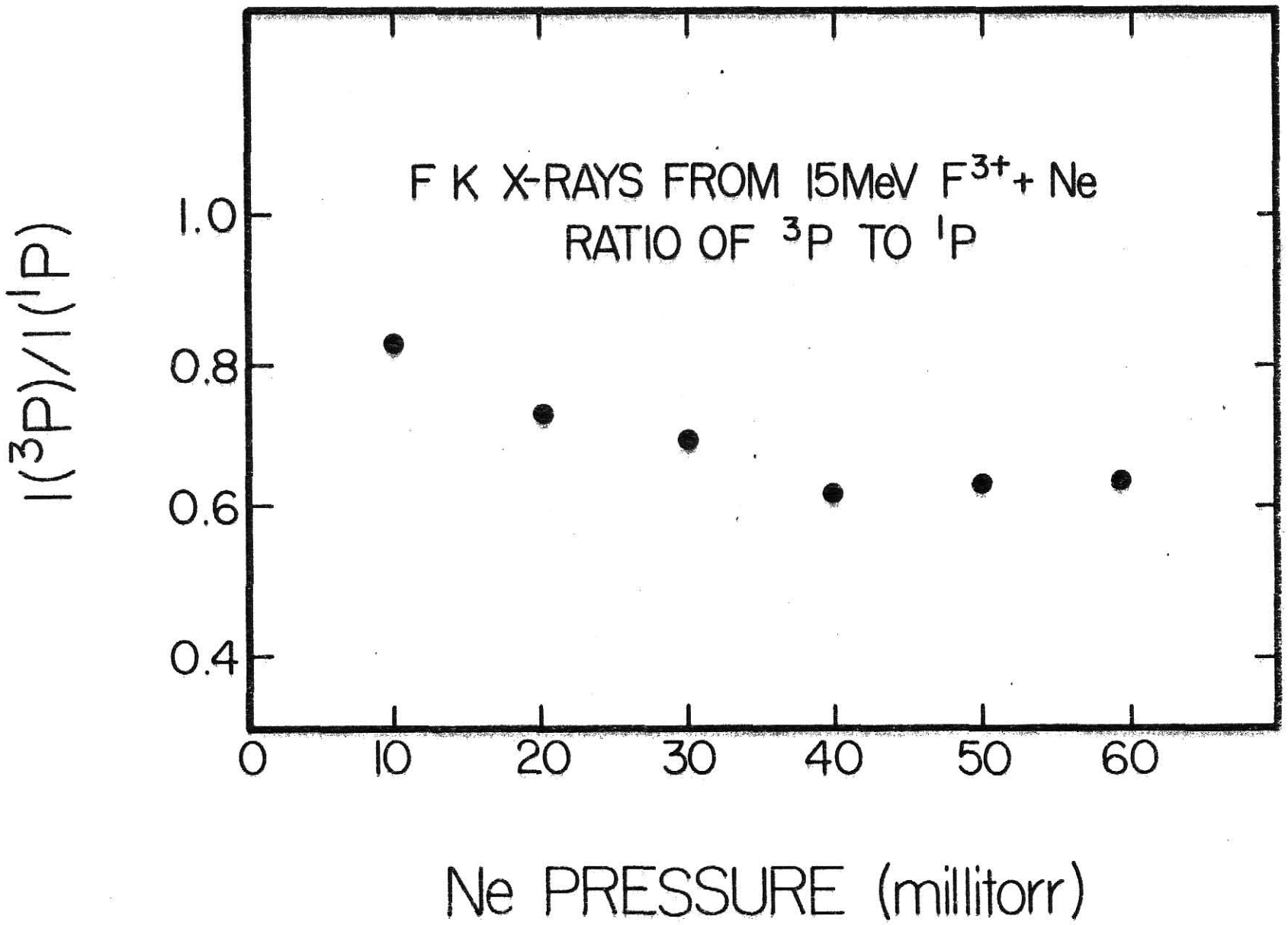
F K X-RAYS FROM 15MeV F^{3+} + Ne
RATIO OF ^3P TO ^1P
$I(^3P)/I(^1P)$
1.0
0.8
0.6
0.4
0
10
20
30
40
50
60
Ne PRESSURE (millitorr)

Figure 8: F K X-ray spectra from F^{q+} on Ne ($2 \leq q \leq 6$)

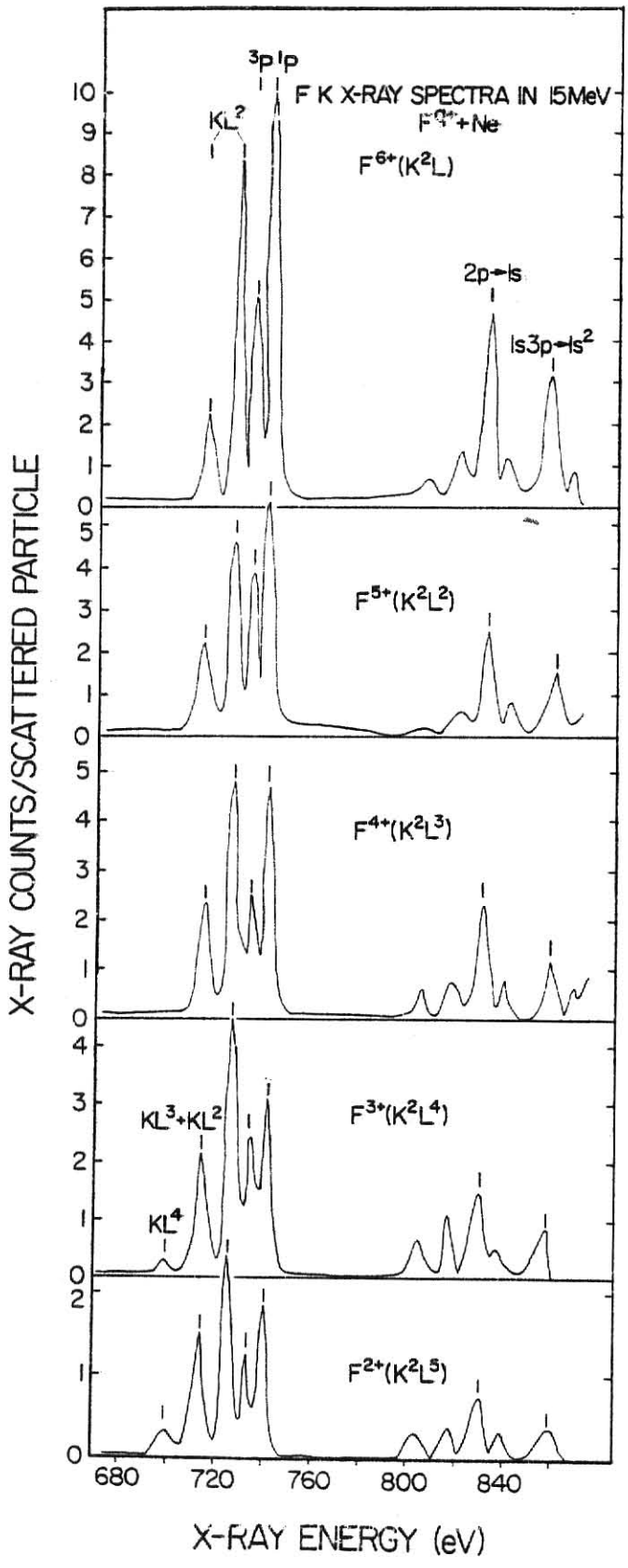
F K X-RAY SPECTRA IN 15MeV
F9+ + Ne
3p 1p
KL2
F6+(K2L)
2p→1s
1s3p→1s2
F5+(K2L2)
F4+(K2L3)
KL3+KL2
KL4
F3+(K2L4)
F2+(K2L5)
X-RAY COUNTS/SCATTERED PARTICLE
X-RAY ENERGY (eV)
680
720
760
800
840

Figure 9: F K X-ray spectra from F^{q+} on Ne ($7 \leq q \leq 9$)

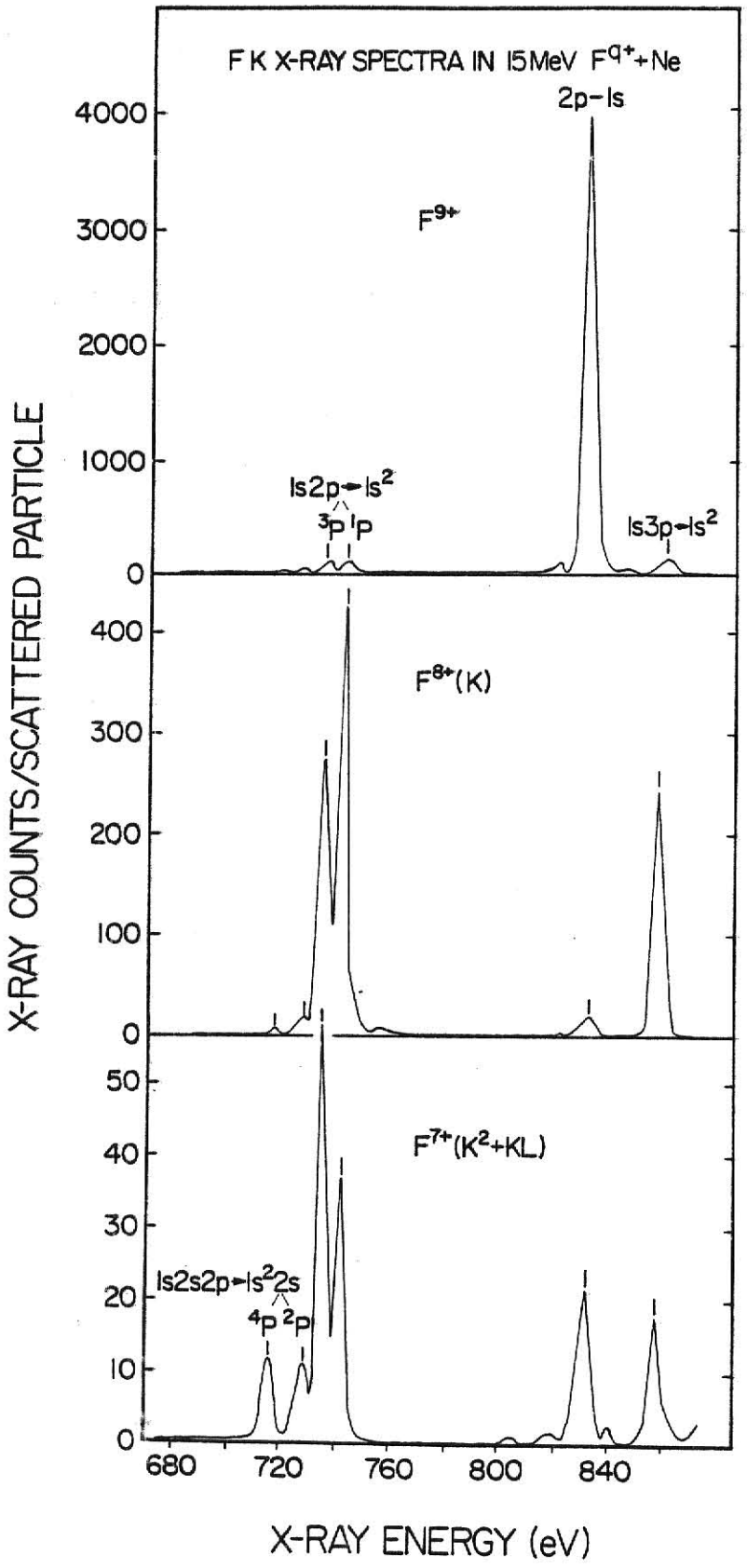
F K X-RAY SPECTRA IN 15 MeV F^{q+}+Ne
2p-1s
F^{9+}
1s2p→1s²
^3P ^1P
1s3p→1s²
F^{8+}(K)
F^{7+}(K^2+KL)
1s2s2p→1s²2s
^4P ^2P
X-RAY COUNTS/SCATTERED PARTICLE
X-RAY ENERGY (eV)
4000
3000
2000
1000
0
400
300
200
100
0
50
40
30
20
10
0
680
720
760
800
840

be formed by two processes, one K-shell and two L-shell electron ionization gives a ($1s2s^2 2p$) intermediate state, which decays to $1s^2 2s^2$ with an energy of 713 eV. At 714.8 eV is a transition which occurs when a $1s2s2p(^4P)$ term, formed when one K-shell and three L-shell electrons are ionized, and which decays to a $1s^2 2s^1(^2S)$ state. Since there is no method to determine the fractional contribution of the processes in this experiment, this ambiguity will persist throughout and the assignment of the dominant transition occurring being based solely on the surrounding peaks. At very low incident charge states, it is presumed that the transition requiring the fewer number of ionized electrons would be preferred. The dominant peak in the 2+ spectrum, at an energy of 725 eV results from a single K-shell and three L-shell electrons being ionized, leaving an intermediate $1s2s2p(^2P)$ term which decays to $1s^2 2s(^2S)$. The next two peaks both result from helium-like emitting ions, as one K-shell and four L-shell electrons are ionized leaving the $1s2p(^3P)$ and $1s2p(^1P)$ terms, Both decay to a $1s^2$ ground state with energies of 731 and 738 eV, respectively. The highest energy peak in the 2+ spectrum, at 858 eV, is another helium-like transition, coming from an intermediate 1s3p configuration. The most intense peak in the high energy region is due to double K-shell, quadruple L-shell ionization, leaving a hydrogenic 2p electron to decay with an energy of 827 eV. The peaks surrounding the hydrogenic transition are believed to be due to doubly excited states of 2, 3, and 4 electron systems as previously shown by Tawara.[19]

$$F^{3+} \ (1s^2 2s^2 2p^2)$$

The peaks in the 3+ spectrum correspond to those in the F^{2+} spectrum, but require one less L-shell electron ionized to produce.

F^{4+} ($1s^2 2s^2 2p^1$)

Here, there are two fewer L-shell electrons to be ionized to obtain the intermediate configurations resulting in a gradual increase in the intensities of all, but the $1s2s^2 2p^2$ to $1s^2 2s^2 2p$ line has become indistinguishable from the background. With this trend toward more highly ionized final charge states, it is expected that the $1s2s2s(^4P)$ fraction is roughly greater than or equal to the $1s2s^2 2p$ configuration.

F^{5+} ($1s^2 2s^2$)

A F^{5+} incident beam has no electrons in the 2p orbital, but every peak in the spectrum depends on electron excitation or electron capture to the 2p level. This indicates that there is probably substantial mixing of the 2s and 2p orbitals during the collision. The first peak is due to the sum of 1s electron excitation to $1s2s^2 2p$, and either K-shell ionization and 2s to 2p electron excitation, or 1s to 2p electron excitation and 2s ionization to a $1s2s2p(^4P)$ intermediate term. All three of the helium-like peaks have occurred due to single electron excitation, and double ionization resulting in $1s2p(^3P)$, and 1s2p terms which decay to the $1s^2$ ground state.

F^{6+} ($1s^2 2s$)

The F^{6+} spectrum follows immediately from the F^{5+}, requiring one less electron ionized. It becomes apparent that the peak at 715 eV is due virtually totally to the (^4P) term because to form a $1s2s^2 2p$ configuration would require 1s electron excitation and a captured electron, and capture processes are not favored due to the low charge state of the ion, as evidenced by the disappearance of the $1s2s^2 2p^2$ to $1s^2 2s^2 2p$ line.

F^{7+} ($1s^2 1s2s$)

The F^{7+} beam arrives on target with some fraction of the ions in a $1s2s(^3S)$ metastable state produced in the poststripper foil. This metastable fraction manifests itself in two places, the $1s2s2p(^4P)$ and the $1s2p(^3P)$ terms. The ^4P state is formed by direct electron capture to the 2p shell of the metastable component of the beam. The ^3P term is formed by direct Coulomb electron excitation of the metastable fraction. These processes involving the metastable fraction result in the $^3P/^1P$ and $^4P/^2P$ ratios being greater than unity for the only time in this charge state study.

F^{8+} (1s)

Single electron capture into the 2p orbital accounts for all of the dominant peaks in this spectrum. An electron captured into the 2p subshell with spin either parallel or antiparallel to the 1s electron results in the $1s2p(^3P)$ and (^1P) terms. Electron capture to the 3p subshell results in the 1s3p configuration present in the high energy region. The capture of two electrons is required to form the lithium-like states barely visible, and electron excitation leads to the hydrogenic 2p - 1s line.

F^{9+} (bare ion)

Bare projectile spectra are particularly simple to explain since all transitions are due to electron capture. Single electron capture to a hydrogenic ion, double capture to a helium-like ion, and triple capture to a lithium-like ion are all observed.

Total Cross Sections

The data obtained by each particular spectrometer scan had to be compared to the data obtained from other scans taken at the same and different charge states. For this intra-experiment normalization the surface barrier detector installed within the interaction region provided the best comparison. The number of particles scattering into this detector in the energy window selected gives an accurate measure of the product of the number of incident particles times the number of Neon atoms contained within the gas cell. This value depends only on nuclear elastic scattering so it is independent of all atomic processes, including the incident ion charge state. To normalize these relative yields to absolute cross sections the data for the 15 MeV 3^+ incident beam was scaled to the previous work of Woods[22] who measured Auger production cross sections of fluorine on neon. The fluorescence yields calculated by Tunnell[23] were utilized to give the total cross sections for various final states. In Table 1 and Fig. 10 the fluorine K x-ray cross sections are shown as a function of the incident ion charge state. When this data is divided by the fluorescence yields calculated by Tunnell, the total cross sections for the production of various final states are obtained. These results are tabulated in Table 2 and shown in Fig. 11. In the tables the charge state of the incident ion is shown in the first column and the configuration of the emitting ion appears in the first row. The various symbols used in Figures 10 and 11 represent the incident charge states, and the abscissa shows the configuration of the ion emitting the x-ray.

Figure 10: F K X-ray cross sections

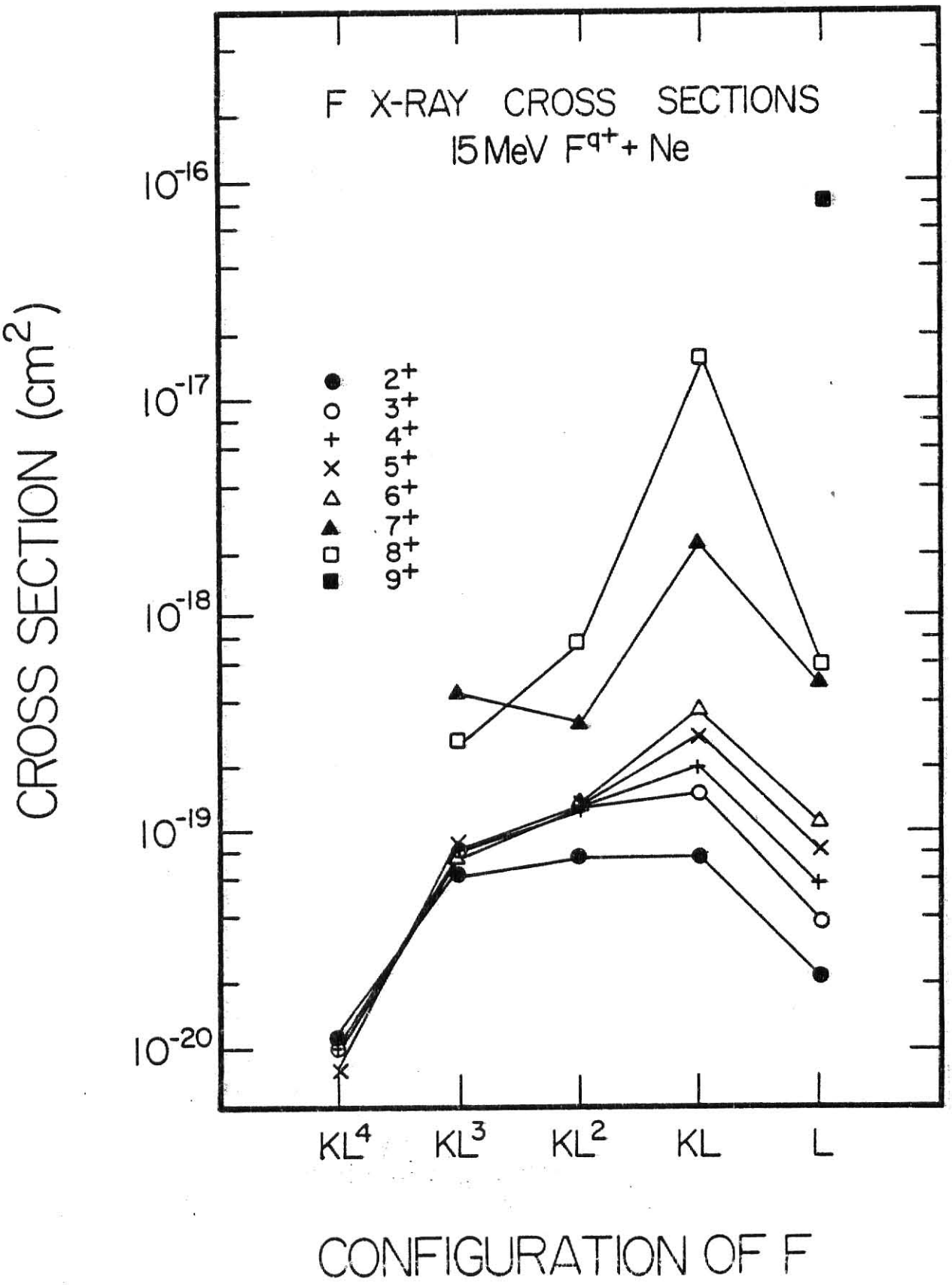
F X-RAY CROSS SECTIONS
15 MeV F^{q+} + Ne
CROSS SECTION (cm^2)
10^{-16}
10^{-17}
10^{-18}
10^{-19}
10^{-20}
2^+
3^+
4^+
5^+
6^+
7^+
8^+
9^+
KL^4
KL^3
KL^2
KL
L
CONFIGURATION OF F

Figure 11: F vacancy production cross sections

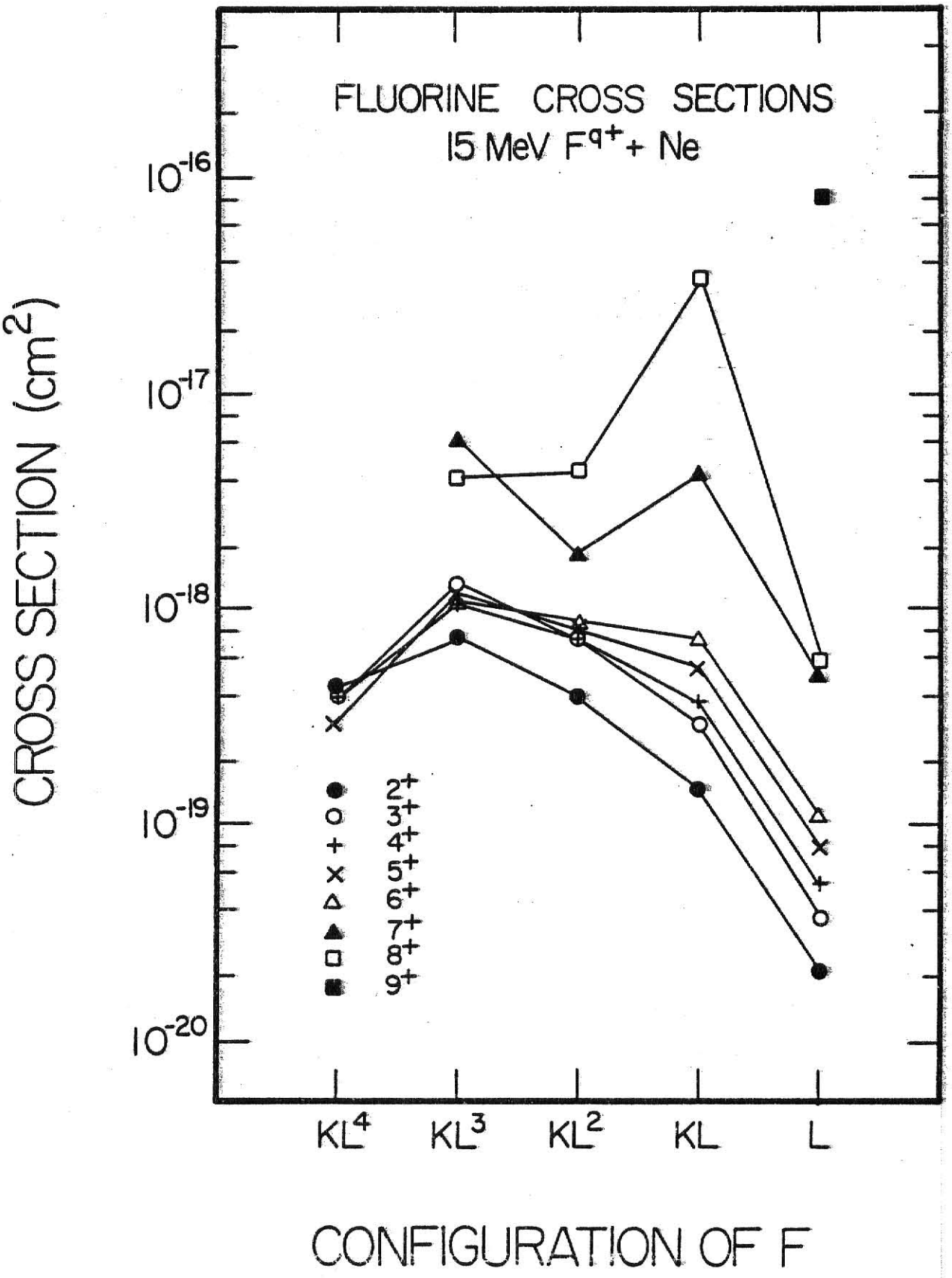
FLUORINE CROSS SECTIONS
15 MeV F^q+ + Ne
CROSS SECTION (cm^2)
10^-16
10^-17
10^-18
10^-19
10^-20
2+
3+
4+
5+
6+
7+
8+
9+
KL^4
KL^3
KL^2
KL
L
CONFIGURATION OF F

Tables 1 and 2: F K X-ray production cross sections and total cross sections

X-Ray Production Cross Sections σ_x (cm^2)

Incident Ion Charge State	Configuration of Emitting Ion				
	KL^4	KL^3	KL^2	KL	L
2^+	1.2×10^{-20}	6.7×10^{-20}	7.9×10^{-20}	7.7×10^{-20}	2.3×10^{-20}
3^+	1.1×10^{-20}	8.1×10^{-20}	1.6×10^{-19}	1.7×10^{-19}	3.8×10^{-20}
4^+	1.1×10^{-20}	8.1×10^{-20}	1.1×10^{-19}	2.0×10^{-19}	5.9×10^{-20}
5^+	8.8×10^{-21}	9.1×10^{-20}	1.6×10^{-19}	2.8×10^{-19}	8.4×10^{-20}
6^+		7.9×10^{-20}	1.7×10^{-19}	3.7×10^{-19}	1.2×10^{-19}
7^+		4.5×10^{-19}	2.8×10^{-19}	2.3×10^{-18}	4.9×10^{-19}
8^+		2.8×10^{-19}	7.9×10^{-19}	1.9×10^{-17}	6.0×10^{-19}
9^+					8.1×10^{-17}

Total Cross Sections $\sigma = \sigma_x / \bar{\omega}$ · (cm^2)

Incident Ion Charge State	Configuration of Emitting Ion				
	KL^4	KL^3	KL^2	KL	L
2^+	4.4×10^{-19}	9.3×10^{-19}	4.1×10^{-19}	1.4×10^{-19}	2.3×10^{-20}
3^+	4.1×10^{-19}	1.1×10^{-18}	8.3×10^{-19}	3.0×10^{-19}	3.8×10^{-20}
4^+	4.1×10^{-19}	1.1×10^{-18}	7.3×10^{-19}	3.6×10^{-19}	5.9×10^{-20}
5^+	3.3×10^{-19}	1.3×10^{-18}	8.3×10^{-19}	5.0×10^{-19}	8.4×10^{-20}
6^+	3.7×10^{-19}	1.1×10^{-18}	8.8×10^{-19}	6.7×10^{-19}	1.2×10^{-19}
7^+		6.3×10^{-18}	1.5×10^{-18}	4.1×10^{-18}	4.9×10^{-19}
8^+		3.9×10^{-18}	4.1×10^{-18}	3.4×10^{-17}	6.0×10^{-19}
9^+					8.1×10^{-17}
Fluorescence Yield ($\bar{\omega} \cdot 100$)	2.68	7.18	19.2	55.4	100

Comparison with Theory

The capture of an electron from an atom to a highly stripped ion is a three body scattering problem which has no formal solution. Among the most widely used quantum mechanical formualtions for electron transfer is the plane wave Born approximation (PWBA), which treats the initial state as a plane wave incident upon a bound electronic target wave function. The final state describes the system as a bound state times a plane wave with one electron having been transferred to the projectile. Within the active electron approximation the roles of all other electrons are ignored. This is reasonable because their main effect is to provide an average screening of the Coulomb forces between the target and projectile nuclei, and between the active electron and the target nucleus. The inclusion of these passive electrons in the theoretical treatment only requires modifying the nuclear charge to an "effective" value. The internuclear Coulomb interaction is neglected in some approximations as it adds only a constant to the total energy, which should not affect the calculated cross sections. When this interaction is omitted from the PWBA the resulting theory is known as the Oppenheimer-Brinkman-Kramers (OBK) approximation. The OBK approximation can be expressed in a simple form if one is willing to limit the focus to the principal quantum numbers of the initial and final states. Such an expression, given by McDowell and Coleman,[26] was used to obtain the theoretical cross sections for electron capture compared with experiment as shown below:

	Incident Charge State	
	8^+	9^+
experiment(cm^2)	3.4×10^{-17}	8.1×10^{-17}
theory(cm^2)	5.8×10^{-16}	1.3×10^{-15}

The theory gives cross sections higher than experiment by a factor of approximately 16, which is normal for this formulation.

The excitation of an ionic electron after the ion's interaction with an atom can also be described theoretically by the Born approximation. The initial and final states are both expressed as plane waves in collision with a bound electron. During the collision the electron gains sufficient energy to excite it to a higher level without gaining enough energy to ionize it. This formulation was used by Bates[27] to obtain an analytical expression for the electron excitation cross sections of an incident one electron ion on unscreened and screened target atoms. The comparison of this theory with experiment is shown below.

	1s → 2p Excitation		
		Theory	
	experiment	unscreened	screened
cross section(cm^2)	6.0×10^{-19}	2.3×10^{-18}	1.7×10^{-18}

VI. CONCLUSION

The purpose of this experiment has been to measure the cross sections for various K-shell interatomic processes as a function of the incident charge state of the fluorine ion. It is hoped that systematic studies of this nature will contribute to the understanding of electron excitation, ionization, and electron capture processes in heavy ion-atom collisions.

Various charge states of a 15 MeV fluorine beam were selected and directed onto a neon gas target. The fluorine K x rays resulting from electron excitation, ionization, or electron capture were detected by a high resolution Bragg crystal spectrometer. The spectra resulting from these measurements showed increases in the K x-ray yield of the fluorine ions, being gradual at first, then quite pronounced as the incident ion arrived with one or more K-shell holes.

Part of the previous work of Tawara[18] is shown in figure 12, where the cross sections for producing the hydrogenic 2p state of fluorine in 15 MeV F^{q+} on He collisions are depicted as a function of the incident ion charge state. The present work, 15 MeV F^{q+} on Ne, is represented by circles; the triangles show the data obtained by Tawara. The data for the incident F^{7+} beam is not plotted due to the ambiguity presented by the metastable portion of the beam. In general the F^{q+} on Ne collisions produce much higher multiple ionization than the F^{q+} on He for the low q projectiles and produce much larger x-ray yields for single electron processes for the high q projectiles. The solid lines are drawn to emphasize the pronounced exponential dependence of the cross sections for producing the 2p final state as the degree of multiple ionization of the incident ions' L shell is increased. This exponential dependence

Figure 12: Production cross sections for the (2p) state of F^{8+} at 15 MeV

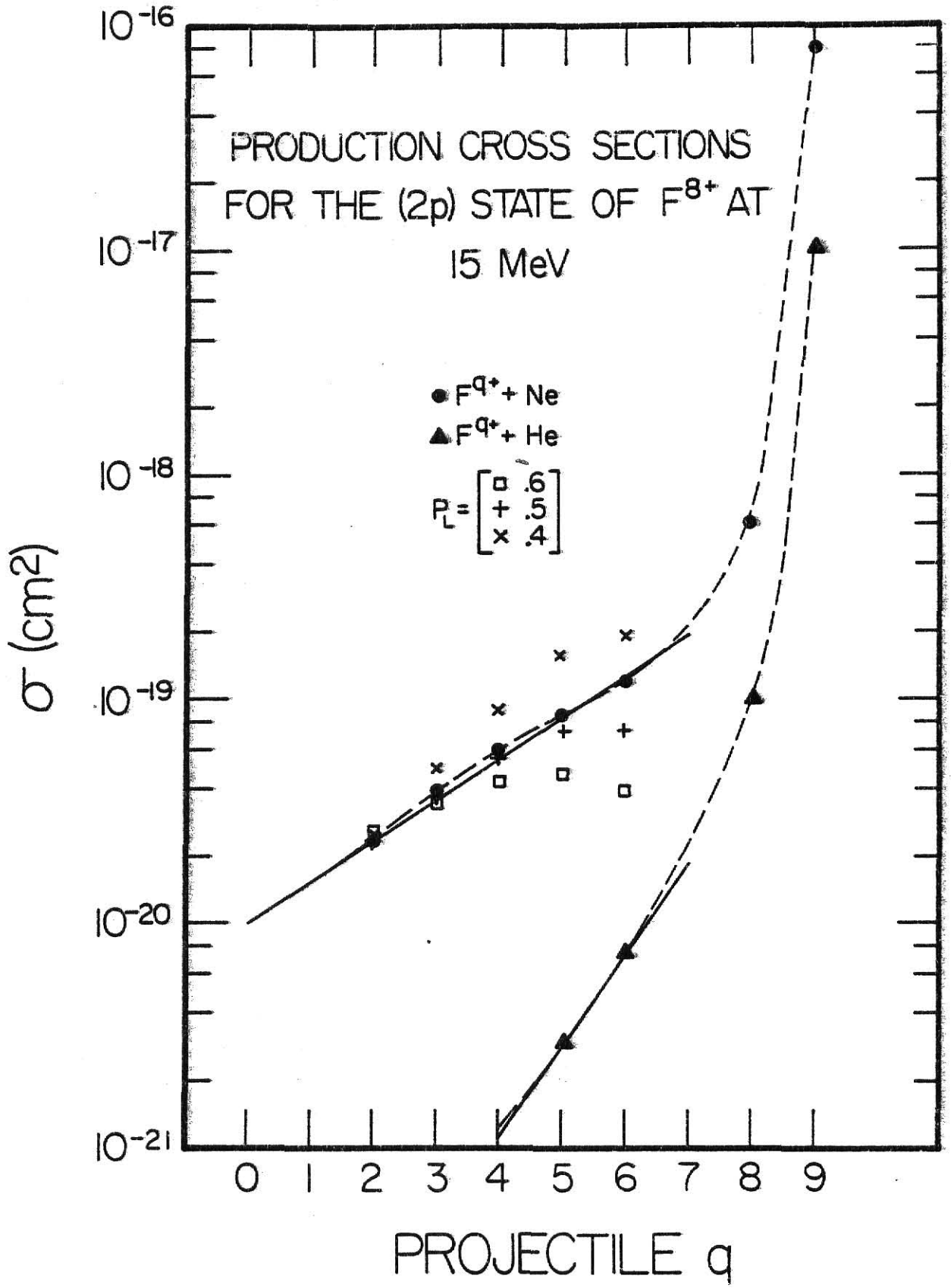
PRODUCTION CROSS SECTIONS
FOR THE (2p) STATE OF F^{8+} AT
15 MeV
F^{q+} + Ne
F^{q+} + He
P_L = .6 .5 .4
σ (cm²)
10^{-16}
10^{-17}
10^{-18}
10^{-19}
10^{-20}
10^{-21}
0 1 2 3 4 5 6 7 8 9
PROJECTILE q

can be explained over a limited range of incident ion charge states by a binomial function of the form

$$A \binom{\ell}{n} P_L^n (1 - P_L)^{\ell-n}$$

which represents the probability of removing n of ℓ electrons. $\binom{\ell}{n}$ is the standard binomial coefficient and A is the normalization constant. Using the above equator, it can be shown that the probability of exciting the 2p state of F^{8+} for an incident projectile of F^{q+} is given by

$$\ell P_L^{(\ell-1)} (1 - P_L) = (7 - q) P_L^{(6-q)} (1 - P_L)$$

Fig. 12 shows the comparison between this experiment and three sets of points corresponding to P_L equal to .6, .5, and .4. It is seen that the binomial expansion approximates the exponential dependence for a limited range of q for $P_L \approx .5$. An inherent advantage in this type of comparison is that some of the normal problems of spectral comparison, such as fluorescence yields and crystal reflectivity, do not occur in this analysis of the data.

It is believed that further study of the systematics of the charge state dependence of fluorine on gaseous targets would be advantageous and should take two possible courses. An energy dependence study of fluorine on neon would be valuable in charting electron excitation, ionization, and electron capture processes as the velocity of the incident ion is changed. A second course of study would be to change the target gas such as argon or krypton. Studies of this kind would complement this thesis and the previous work of Tawara.

REFERENCES

1. W. M. Coates, Phys. Rev. 46, 542 (1934).
2. H. G. Mosley, Phil. Mag. 26, 1024 (1913); Ibid. 27, 703 (1914).
3. H. J. Specht, Z. Phys. 185, 301 (1965).
4. P. Richard, I. L. Morgan, T. Furuta and D. Burch, Phys. Rev. Letters 23, 1009 (1969).
5. D. Burch and P. Richard, Phys. Rev. Letters 25, 983 (1970).
6. A. R. Knudson, D. J. Nagel and P. G. Burkhalter, Phys. Letters 42A, 69 (1972).
7. D. Burch, P. Richard and R. L. Blake, Phys. Rev. Letters 26, 1355 (1971)
8. P. G. Burkhalter, A. R. Knudson, D. J. Nagel and K. L. Dunning, Phys. Rev. A 6, 2093 (1972).
9. R. L. Watson, A. K. Leeper, B. I. Sonobe, T. Chiao and F. E. Jenson, Phys. Rev. A 15, 914 (1977).
10. C. F. Moore, D. L. Matthews and H. H. Wolter, Phys. Letters 54A, 407 (1975).
11. F. Hopkins, J. Sokolov and A. Little, Phys. Rev. A 14, 1907 (1976).
12. C. Schmiedekamp, B. L. Doyle, T. J. Gray, R. K. Gardner, K. A. Jamison and P. Richard, Phys. Rev. A 18, 1892 (1978).
13. R. L. Kauffman, K. A. Jamison, P. Richard and T. J. Gray, Phys. Rev. Letters 36, 1074 (1976).
14. H. Tawara, P. Richard, T. J. Gray, P. Pepmiller, J. R. Macdonald and R. Dillingham, Phys. Rev. A 19, 2131 (1979).
15. L. M. Winters, J. R. Macdonald, M. D. Brown, T. Chiao, L. D. Ellsworth and E. W. Pettus, Phys. Rev. A 8, 1835 (1973).

16. J. R. Mowat, I. A. Sellin, P. M. Griffin, D. J. Pegg and R. S. Peterson, Phys. Rev. A 9, 644 (1974).

17. F. Hopkins, R. L. Kauffman, C. W. Woods and P. Richard, Phys. Rev. A 9, 2413 (1974).

18. H. Tawara, P. Richard, K. A. Jamison, T. J. Gray, J. Newcomb and C. Schmiedekamp, Phys. Rev. A 19, 1960 (1979).

19. M. A. Blohkin, Methods of X-Ray Spectroscopic Research, edited by M. A. S. Ross (Pergamon Press, 1965) p. 176.

20. R. J. Fortner and D. L. Matthews, Phys. Rev. A 16, 1441 (1977).

21. R. L. Kauffman, C. W. Woods, F. F. Hopkins, D. O. Elliott, K. A. Jamison and P. Richard, J. Phys. B 6, 2197 (1973).

22. C. W. Woods, R. L. Kauffman, K. A. Jamison, N. Stolterfoht and P. Richard, Phys. Rev. A 13, 1358 (1976).

23. T. W. Tunnell, C. Can and C. P. Bhalla, IEEE Transactions on Nuclear Science, NS-26, 1124 (1979).

24. J. R. Oppenheimer, Phys. Rev. 31, 349 (1928).

25. H. C. Brinkman and H. A. Kramers, Proc. Acad. Sci. Amsterdam 33, 973 (1930).

26. M. R. C. McDowell and J. P. Coleman, Introduction to the Theory of Ion-Atom Collisions, (North-Holland Publishing Co., N. Y., 1970) p. 379.

27. D. R. Bates, Atomic and Molecular Processes, edited by D. R. Bates (Academic Press, N. Y., 1962) p. 550.

CHARGE STATE STUDY OF FLUORINE K X RAYS FOLLOWING A FLUORINE-NEON COLLISION

by

PHILIP L. PEPMILLER

B.S., Florida State University, 1977

AN ABSTRACT OF A MASTER'S THESIS

submitted in partial fulfillment of the

requirements for the degree

MASTER OF SCIENCE

Department of Physics

KANSAS STATE UNIVERSITY
Manhattan, Kansas

1980

ABSTRACT

Fluorine beams at an energy of 15 MeV with charge states from 2^+ through 9^+ were obtained from the Kansas State University tandem Van de Graaff accelerator and directed onto a neon gas target operated at pressures between 10 and 60 millitorr. The fluorine K x rays resulting from the F - Ne collisions were detected by a Bragg crystal spectrometer with an energy resolution of 4 eV. The resolved x-ray peaks were identified with the processes of single and multiple electron excitation, ionization and electron capture for each incident ion charge state. The resulting x ray yields were converted to cross sections by normalizing to previous total Auger electron measurements of F - Ne collisions. The cross sections for forming given final states are observed to increase in an experimental manner as the charge state of the incident ion is varied from 2^+ through 6^+. For the incident projectiles with one or more K-shell vacancies the cross sections for certain final states increase dramatically over those of the low charge state ions. The cross sections for the one-electron processes of excitation and capture are compared with existing Born approximation calculations.